PROCEEDINGS OF SCIENCE

VERITAS Observations of Mrk 421 in Jan-Feb 2008 with Simultaneous Coverage in the X-ray Band

Luis C. Reyes[*a] **for the VERITAS**[b] **Collaboration**

[a] *Kavli Institute for Cosmological Physics at the University of Chicago*
533 E 56th St, Chicago, IL 60637
[b] *See http://veritas.sao.arizona.edu for a full list of authors*

The TeV blazar Mrk 421 has been observed in an active state in January and February 2008 by the VERITAS gamma-ray observatory. Simultaneous X-ray observations have been obtained with Swift-XRT and RXTE. In this contribution we present the light curves obtained in both energy bands and their correlation.

Workshop on Blazar Variability across the Electromagnetic Spectrum
April 22-25 2008
Palaiseau, France

[*] Speaker.

PoS(BLAZARS2008)057

1. Introduction

Mrk 421 ($z = 0.030$) is a remarkable astrophysical object: it is the brightest BL Lac object at X-ray and UV-wavelengths and it was the first extragalactic source discovered at TeV energies [18]. Furthermore, strong variability has been observed in this source at X-ray and TeV energies with timescales from less than an hour [2, 8] to years [5].

Mrk 421 is a blazar, and as other Active Galactic Nuclei (AGN), blazars are thought to be powered by the release of gravitational energy by accretion of material into a supermassive black hole located in the central region of the host galaxy [22]. Some AGN present strong relativistic outflows in the form of jets, with blazars being the particular subset whose jets are aligned with our line of sight. Similarly to other blazars, the spectral energy distribution (SED) of Mrk 421 shows two pronounced peaks (see [7] for SED details), which suggests at least two different physical emission processes at play. The first bump (extending from radio to X-rays) is widely thought to be due to polarized synchrotron emission from high energy electrons, while different emission models (briefly introduced below) have been proposed to explain the second energy bump, which extends up to TeV energies. It should be noted that the high-energy emission component dominates the bolometric luminosity of this source, a powerful demonstration of the extreme nature of this type of source.

The models that have been proposed to explain gamma-ray emission in blazars can be roughly categorized into leptonic and hadronic mechanisms, depending on whether the accelerated particles responsible for the gamma-ray emission are primarily electrons/positrons or protons. In leptonic models, high-energy electrons/positrons produce gamma rays via Inverse Compton scattering of low-energy photons. In Synchrotron Self-Compton (SSC) models, the same population of electrons responsible for the observed gamma rays generates the low-energy photon field through synchrotron emission. In External Compton (EC) models the low-energy photons originate outside the jet. Possible sources of external photons include: accretion disk photons radiated directly into the jet, accretion disk photons scattered by emission-line clouds or dust into the jet, or synchrotron radiation re-scattered back into the jet by broad-line emission clouds. In hadronic models gamma rays are produced by high-energy protons, either via proton synchrotron radiation, or via the interaction of high-energy protons with ambient photons (see [3, 23] and references therein for a review of blazar gamma-ray emission processes).

Different models for the high-energy emission properties of blazars have distinct observational signatures, which can in principle be revealed with sufficiently accurate time-resolved broadband spectroscopy and correlated variability studies. Of particular importance for the observations presented in this paper, a strong linear correlation between X-ray and TeV fluxes is expected for inverse Compton emission models, since the same electron population is responsible for both the synchrotron and high-energy emissions[20].

In this contribution we present the TeV and X-ray observations obtained for Mrk 421 in early 2008 and their correlation.

2. VERITAS Observations

The VERITAS (Very Energetic Radiation Imaging Telescope Array System) is an array of four

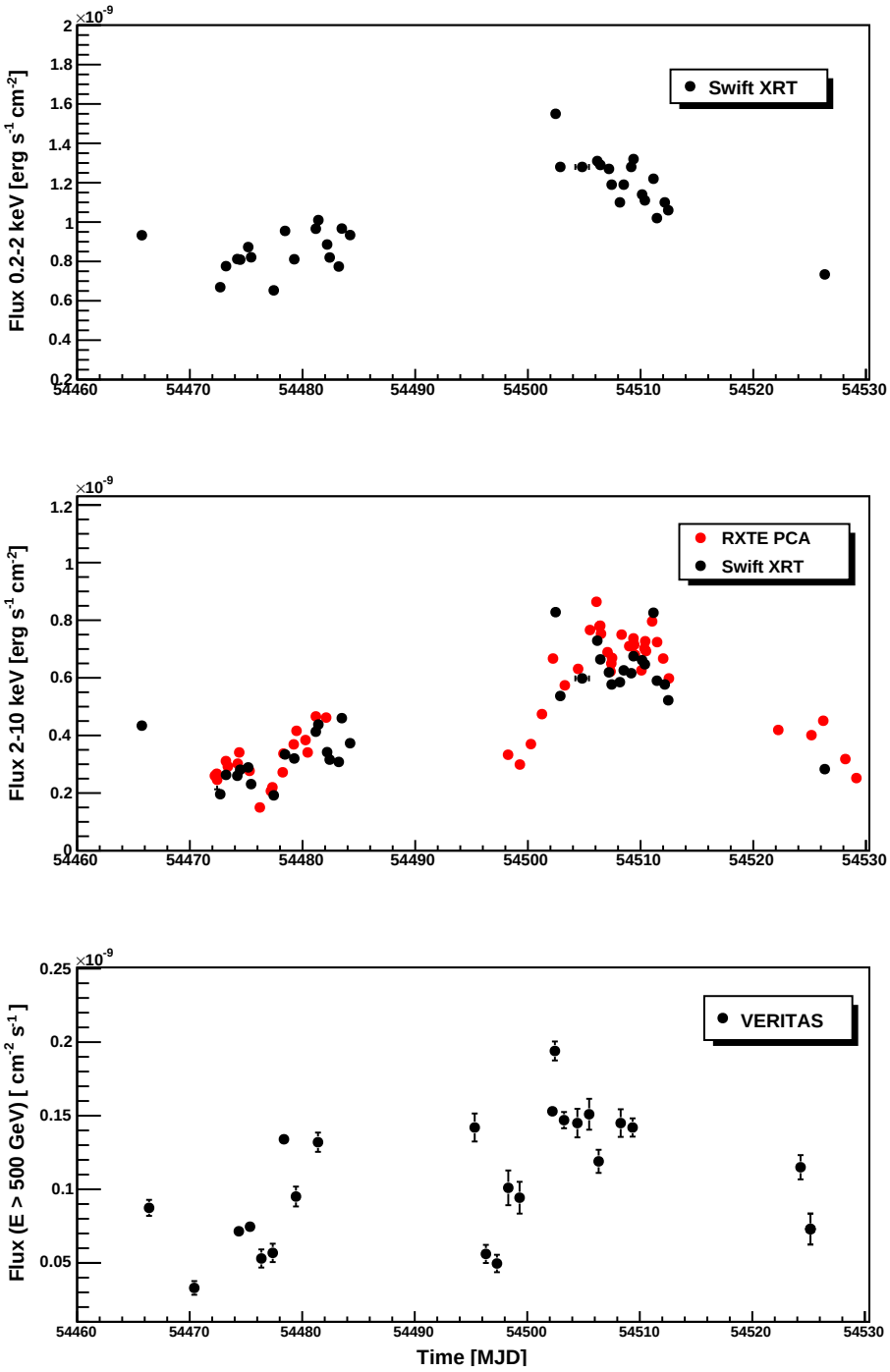

Figure 1: Top panel: Lightcurve of soft X-rays (0.2 - 2 keV) from Swift XRT. Middle panel: Lightcurve of hard X-rays (2 - 10 keV) from Swift XRT (red points) and RXTE PCA (black points). For these two panels the flux error bars are smaller than the symbols. Bottom panel: Integral flux above 500 GeV measured by VERITAS

12m diameter imaging atmospheric Cherenkov telescopes (IACTs) in southern Arizona, U.S.A. [24]. In each telescope, a fraction of the Cherenkov light produced by gamma rays (and cosmic rays) interacting in the atmosphere is collected into a camera that consists of 499 photo-multiplier-tubes (PMTs). The PMTs in each camera are separated by 0.15°, and together, they cover a 3.5° field of view. The combination of optical and electronic systems in VERITAS allows imaging of the shower and its development with an angular resolution of 0.1° and a time resolution of 2 ns (see [1, 12, 15] for a detailed description of the hardware system and the performance of the VERITAS observatory).

Data reduction of these observations followed the methods described in [1]: The shower image from every camera is parameterized according to the Hillas method [10], and the gamma-ray direction and air shower impact parameter on the ground are then reconstructed using standard stereoscopic techniques [11, 13]. Background events are rejected using selection cuts on the arrival direction, mean scaled width and length, and by using quality cuts for each event. The energy and effective area of each event are reconstructed using lookup tables from Monte Carlo simulations of gamma rays. Furthermore, the events are processed using independent analysis packages, which provide consistent results [6].

The gamma-ray observations described in this document were taken in wobble mode at 0.5° offset during January and February of 2008, for a total of ∼15 hours. During this period, the source was found in an active state, with fluxes ranging from ∼0.5 Crab to ∼2 Crab (as shown in the bottom panel of figure 1). The ability of VERITAS to obtain flux measurements such as those shown in the figure(with as little as 10 minutes of exposure in some nights) highlights the sensitivity and scientific potential of VERITAS for ongoing and future multi-wavelength campaigns.

3. X-ray Observations

3.1 RXTE PCA Data

A total of 44 RXTE PCA observations (60 ks) were analyzed with standard HEASOFT tools. The data were fitted with a power law model and fixing the hydrogen column density to its galactic value: $n_H = 1.61 \times 10^{20}$ cm^{-2} (as measured by Lockman & Savage [14]). As can be appreciated in the middle panel of figure 1, a factor of >3 increase in the X-ray flux was observed in early February. This was coincident with the increase at TeV energies. The distribution of flux vs. spectral index (bottom left plot in figure 2) shows a clear correlation and a noticeable width. Deviations from a perfect straight line are particularly interesting (since they may account for spectral variability of the accelerated particles, signatures of Fermi acceleration, radiative cooling and/or variable energy cutoffs). A detailed analysis of these deviations is underway.

3.2 Swift XRT Data

The data considered in this document accounts for a total of 34 Swift XRT observations (or about 45 ks), which were analyzed with standard HEASOFT tools. As is common for Swift XRT observations of Mrk 421, all data were taken in Windowed Timing (WT) mode. The data were fitted in the energy range 0.2 - 10 keV using two spectral models (galactic absorption is applied in

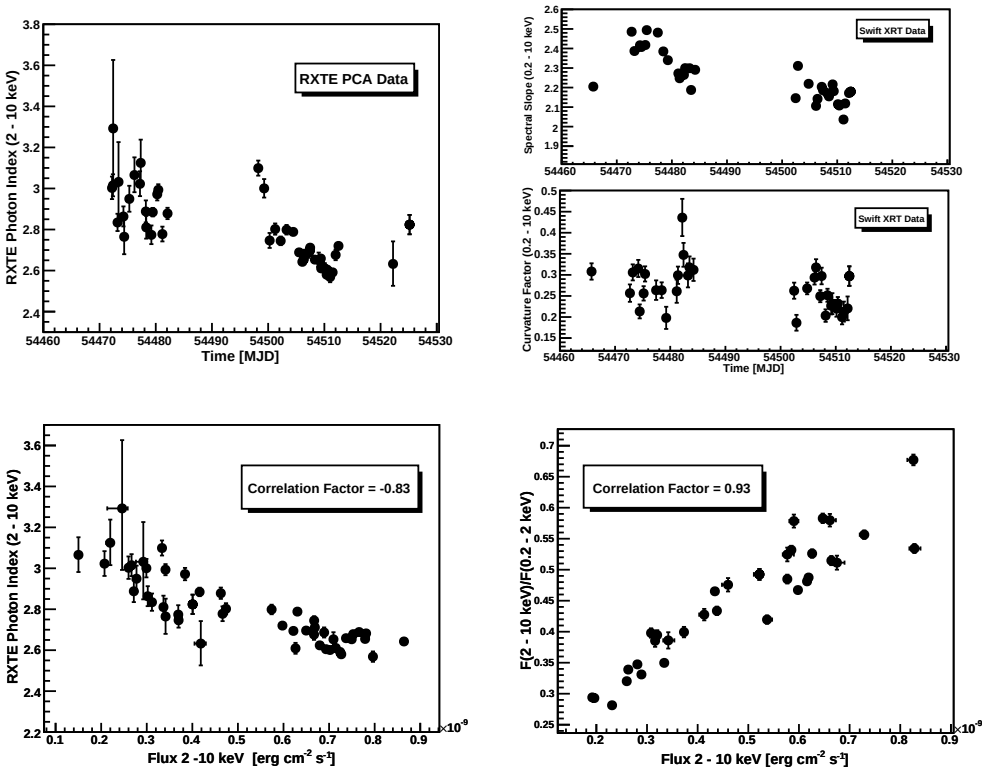

Figure 2: Top left panel: Photon spectral index measured by RXTE-PCA for each observation. The strong anticorrelation of the spectral index with the total flux is evident in the bottom left figure. The spectral slope and curvature factors (i.e. a and b in eq. 3.1)are shown in the top and middle right panels respectively. It should be noted that the curvature factor is significantly inconsistent with zero (as would be the case for a spectrum that can be appropriately described by a power law fit). The bottom right plot presents the strong correlation between the flux ratio of hard (2-10 keV) to soft (0.2-2 keV) X-rays and the hard X-ray flux. The correlation factors shown in the figure follow the definition by Pearson [17] (see [21] for details).

each case): i) a simple power law, and ii) a log-parabola:

$$F(E) = kE^{-(a+b\log E)} \tag{3.1}$$

Consistent with the results by Tramacere et al 2007 [21], we find that a log-parabola model improves the χ^2 statistic and yields fit residuals with no systematic deviations. Only those results obtained with the log-parabola model are presented here. The spectral slope factor a and the curvature factor b from eq. 3.1 obtained for each observation are shown in the top and middle right plots of figure 2. It should be noted that for all observations, the spectral curvature factor (b) is statistically inconsistent with zero. This supports the interpretation of intrinsic curvature at the source [21].

Swift XRT's large bandpass allows us to calculate the X-ray flux in two different energy bands: 0.2 - 2 keV and 2 - 10 keV (top and middle plots in figure 1), and its hardness ratio (see bottom right plot in figure 2). We find that: i) the source is more variable in the hard X-rays than soft X-

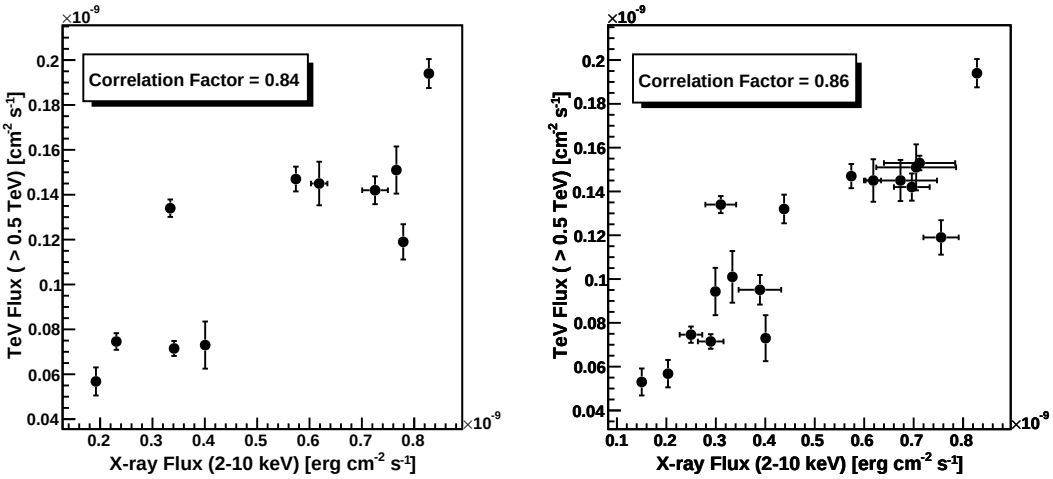

Figure 3: VERITAS TeV flux vs. X-ray flux. The left plot presents the data pairs from simultaneous observations. The right plot presents the same after relaxing the simultaneity requirement by ~ 5 hours (in either time direction). When more than one X-ray observation is available for a given TeV observation, the average X-ray flux is used in the plot. The correlation factors shown in the figure follow the definition by Pearson [17] (see [21] for a details).

rays, and ii) the source gets harder with increasing flux. Both findings are consistent with previous observations (e.g. Brinkmann et al 2001 [4]).

4. Correlation of TeV and X-ray Fluxes

Combining the Swift XRT and RXTE data we obtain 11 pairs of overlapping TeV, X-ray observations that are truly simultaneous. As can be appreciated in the left plot of figure 3, the TeV flux shows a strong linear correlation with the X-ray flux.

Relaxing the simultaneity requirement by 5 hours (in either time direction), we end up with 18 pairs of observations (right plot in figure 3). When more than one X-ray observation is available the average X-ray flux is used in the plot. In this case the linear correlation between the TeV and X-ray flux is also evident.

5. Conclusions

Mrk 421 was observed in an active state during January and February 2008 by the VERITAS gamma-ray telescope with contemporaneous (sometimes truly simultaneous) observations in the X-ray band with Swift XRT and RXTE. The linear correlation between the TeV and X-ray fluxes reported in previous studies [7, 9, 16, 19] is confirmed by these observations. This favors SSC models where the same electron population is responsible for the synchrotron and high-energy emission observed in this blazar.

The good quality lightcurves and spectral information obtained by VERITAS and the X-ray telescopes constitute a rich data sample to probe blazar models of particle acceleration and high-

energy emission. The results presented in this contribution are purely a nigh-by-night variability study of Mrk 421 at TeV and X-ray energies. A more detailed analysis of these data, considering shorter time scale variability and additional data taken during March-May 2008 is underway.

Acknowledgements

This research is supported by grants from the U.S. Department of Energy, the U.S. National Science Foundation, and the Smithsonian Institution, by NSERC in Canada, by PPARC in the UK and by Science Foundation Ireland. We acknowledge the great support by the Swift XRT team. In particular we wish to thank Neil Gehrels and Abe Falcone for their support for observations of TeV blazars. Luis Reyes acknowledges the support by the Kavli Institute for Cosmological Physics at the University of Chicago through grants NSF PHY-0114422 and NSF PHY-0551142 and an endowment from the Kavli Foundation and its founder Fred Kavli.

References

[1] V. A. Acciari et al. , *ApJ*, **679**, 1427 (2008)

[2] F. Aharonian et al. *A&A*, **393**, 89 (2002)

[3] M. Boettcher, *ApSS*, **309**, 95 (2007)

[4] W. Brinkmann et al., *A&A*, **365L**, 162 (2001)

[5] W. Cui, *ApJ*, **605**, 662 (2004)

[6] M. Daniel et al., *Proc. 29th International Cosmic Ray Conference*, **OG2.7** (2007)

[7] G. Fossati, J. Buckley et al., *ApJ*, **677**, 906 (2008)

[8] J. A. Gaidos et al., *Nature*, **383**, 319 (1996)

[9] B. Giebels et al., *A&A*, **462**, 29 (2007)

[10] A. M. Hillas, *Proc. 19th International Cosmic Ray Conference*, **3**, 445 (1995)

[11] W. Hofmann et al., *A*stroparticle Physics, **12**, 135 (1999)

[12] J. Holder et al., *Astroparticle Physics*, **25**, 391 (2006)

[13] H. Krawczynski et al., *A*stroparticle Physics, **25**, 380 (2006)

[14] F. J. Lockman & B. D. Savage, *ApJS*, **97**, 1, (1995)

[15] G. Maier et al., *Proc. 29th International Cosmic Ray Conference*, **OG2.7** (2007)

[16] L. Maraschi et al., *ApJ*, **526L**, 81 (1999)

[17] K. Pearson, *Philos. Trans. Royal Soc. London Ser. A* , **187**, 253 (1896)

[18] M. Punch et al., *Nature*, **358**, 477 (1992)

[19] P. F. Rebillot et al., *ApJ*, **641**, 740 (2006)

[20] T. Takahashi, *ApJ*, **470**, 89 (1996)

[21] A. Tramacere et al., *A&A*, **467**, 501 (2007)

[22] C. M. Urry and P. Padovani, *PASP*, **107**, 83 (1995)

[23] C. Von Montigny et al., *ApJ*, **440**, 525 (1995)

[24] T. C. Weekes et al., *Astroparticle Physics*, **17**, 221 (2002)